STRUCTURAL INSIGHTS INTO THE REGULATION OF JAK3 ACTIVITY: EVIDENCE FROM MOLECULAR MODELING OF THE FULL HUMAN JAK3 PROTEIN

An Undergraduate Research Scholars Thesis

by

JAIMIE ALBACH

Submitted to the Undergraduate Research Scholars program at
Texas A&M University
in partial fulfillment of the requirements for the designation as an

UNDERGRADUATE RESEARCH SCHOLAR

Approved by Research Advisor: Dr. Jhenny Galan

May 2017

Major: Marine Biology

TABLE OF CONTENTS

ABSTRACT

Structural insights into the regulation of JAK3 activity: Evidence from molecular modeling of the full human JAK3 protein

Jaimie Albach
Department of Marine Biology
Texas A&M University

Research Advisor: Dr. Jhenny Galan
Department of Marine Sciences
Texas A&M University

JAK3 is a receptor-associated tyrosine kinase that functions a key signal transducer within the JAK-STAT cellular signaling pathway to facilitate the production, proliferation, and differentiation of various cell types. Mutations to JAK3 have been shown to disrupt hematopoietic stem cell signaling, causing abnormalities in immune cell production, linking the protein to various immune-deficiency diseases, inflammatory disorders, and cancers. In this study we provide key information about JAK3 structure that gives crucial insight into the function of the protein at the molecular level, allowing for better understanding of the protein's integral role in cell signaling pathways and immune related disorders. We report two full, theoretical 3D structural models of the JAK3 human protein, encompassing all 7 Jak Homology (JH) protein domains. The kinase domain (JH1), was obtained from the protein data bank (PDBID: 4QPS), while the remaining JH domains were constructed using multi-template homology modeling techniques and molecular dynamics simulations. Sequence alignment revealed conserved homology properties and JAK2 and TYK2 were used as structural templates to model the pseudokinase (JH2) and SH2-FERM (JH3-JH7) domains in JAK3 respectively.

Molecular dynamics simulations served to optimize and merge domain models in phases, one domain at a time by two different pathways, validating the models at each phase using RMSD and energy minimization calculations. The structural and dynamic properties of the protein, including residue interactions, domain-domain modulations, and conformational behavior are quantified. This study is an important step in better understanding JAK3 structure-function mechanisms and molecular interactions and may aid in discovery of novel inhibitors with higher JAK3 selectivity through structure-based drug design.

DEDICATION

I would like to give thanks to my advisor, Dr. Galan, for her patience, effort, and time. I am appreciative of her willingness to help me with any questions or concepts of which I was unsure and the manner with which she did so, comprehensively, patiently, and without a hint of derision. Her presence, support, and confidence in me throughout the years of my undergraduate career were fundamental in my accomplishing many achievements and motivated me to advance in trying times.

ACRONYMS

AMKL	Acute Mega-karyoblastic Leukemia
ATLL	Adult T-cell Leukemia/Lymphoma
BLAST	Basic Local Alignment Search Tool
EMBL-EBI	European Molecular Biology Laboratory- European Bioinformatics Institute
EMBOSS	European Molecular Biology Open Software Suite
FAK	Focal Adhesion Kinase
HSC	Hematopoietic Stem Cells
IL	Interleukin
JAK	Janus Kinase or Just Another Kinase
MD	Molecular Dynamics simulations
MSA	Multiple Sequence Alignment
NAMD	Nanoscale Molecular Dynamics program
NCBI	National Center for Biotechnology Institute
NK	Natural Killer cell
NPT	Constant number molecules/atoms (N), constant pressure (P), and constant temperature (T) ensemble; Isothermal-isobaric ensemble
NVT	Constant number molecules/atoms (N), constant volume (V), and constant temperature (T) ensemble, canonical ensemble
PDB	Protein Data Bank
PDBID	Protein Data Bank Identification number
PW	Pairwise sequence alignment

RMSD	Root-Mean Square Deviation
SCID	Severe Combined Immunodeficiency Disease
STAT	Signal Transducer and Activator of Transcription
T-ALL	T-cell lymphoblastic leukemia
TAMU	Texas A&M University
TYK	Tyrosine Kinase
VMD	Visual Molecular Dynamics

CHAPTER I

BACKGROUND INFORMATION

A protein domain is a characteristic range of amino acid residues with a specific sequence, structure, and function that can be found almost identically or very similarly in related proteins. Though each of the domains of JAK proteins operates independently with unique function, the domains must interact with one another in order to accomplish the overall activity of the protein. Amino acids do not only participate in covalent interactions with their directly adjacent neighbors and intermolecular interactions with slightly distant neighbors to form local secondary structures, but they may also interact with one another on different portions of the protein. Domain-domain interactions influence conformation significantly and contribute to the overall tertiary structure of a protein. Conformational structure therefore is related to domain-domain coordination which changes in response to domain activity to carry out a protein's function. Consequently, protein function is directly tied to protein structure.

Domain structures (along with the primary amino acid sequences) of nearly all the JAK family proteins have been elucidated experimentally, giving key insight into domain-domain modulations and molecular interactions that result in the proteins' functions. However for JAK3, only a structural model of the kinase domain (JH1) has been elucidated experimentally (Goedken, 2015). In order to fully understand the structure-function interactions of JAK3, a full tertiary structural model encompassing the JH1 as well as the JH2, SH2, and FERM domains is essential.

The main objectives of this study are as follows: 1) To generate models of the tertiary structures of the pseudokinase (JH2) domain and SH2-FERM (JH3-JH7) using multi-template

homology modeling and molecular dynamics (MD) simulations. 2) To generate the full model tertiary structures of the JAK3 human protein by combining all protein domains: Kinase (JH1), Pseudokinase (JH2), SH2 (JH3-4), and FERM (JH5-7) in a stepwise fashion using MD simulations. 3) To validate models and quantify domain-domain interactions by examining key residue interactions, such as hydrogen-bonding and salt bridging, among residues at inter-domain interfaces. Model structure validation is accomplished at each phase with RMSD and energy minimization calculations, various pathways of merging domain structures to explore the conformational space, and the identification of functionally significant residues present in our models.

Knowledge of JAK3 structure provides greater insight into JAK3 function at the molecular level furthering understanding of the protein's role in hematopoietic stem cell signaling within the JAK-STAT pathway and the protein's link to various immune deficiency diseases, inflammatory disorders, and cancers.

JAK Structure

Proteins within the same family have similar homology, or high similarity among protein sequence, structure, and overall function. There four members of the Janus Kinase or Just Another Kinase (JAK) protein family: JAK1, JAK2, JAK3, and Tyrosine Kinase 2 (TYK2) (Rane & Reddy, 2000). All four JAK proteins have seven characteristic protein domains termed JH1- JH7 or Janus Homology domains (JH) (Figure. 1).

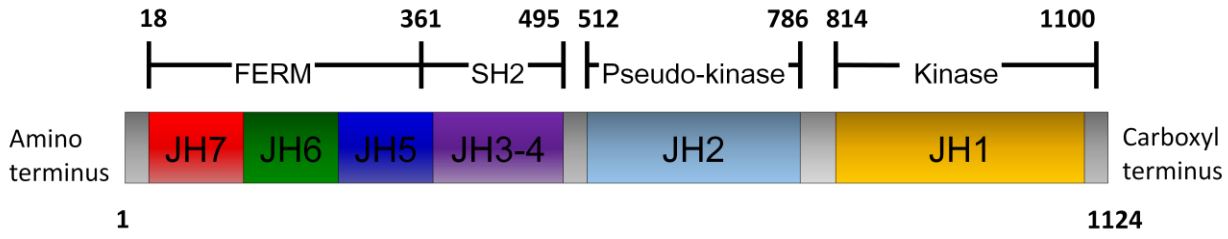

Figure 1. JH7-JH1 domains of JAK family proteins. Relative domain ranges of JAK3 found using NCBI **(**National Center for Biotechnology Institute**)** Protein BLAST (Basic Local Alignment Search Tool) (Altschul, 1990).

The JH domains of JAKS are categorized into four protein domains: FERM, SH2, the Pseudokinase, and the Kinase (Wu & Sun, 2011). The amino acid sequence in JAKs begins with JH7 and continues in descending order to JH1. Beginning with the amino N-terminus, JH7, JH6, and JH5 comprise the three-lobed FERM domain, thought to be the receptor binding region of the protein (Giordanetto & Kroemer, 2002). Following FERM, JH4 and JH3 make up the Src homology 2 (SH2) domain, which functions in facilitating phosphorylation of other proteins by attracting and binding kinase domain containing proteins (Wu & Sun, 2011). A small segment of amino acids follows the SH2 domain linking it to the JH2 domain, or pseudo-kinase domain, followed by an additional domain linker region connecting the JH2 to the JH1. The JAK terminates with JH1, the catalytically active kinase domain, which contains key tyrosine residues needed for JAK phosphorylation (Rane & Reddy, 2000). Short sequences of residues cap the JAK protein at the amino (N-terminus) and carboxyl (C-terminus) ends of the protein.

The JAK-STAT Pathway

The main function of the JAK proteins is to mediate the proliferation and differentiation of different cell types. This is achieved by serving as signal transducers during cellular communication in the cascade of interactions that occur within various signaling pathways (Shuai & Liu, 2003). One of the most important roles of the Janus Kinases is their implication in the JAK-STAT (Janus Kinase-Signal Transducer and Activator of Transcription) signaling pathway (Figure. 2).

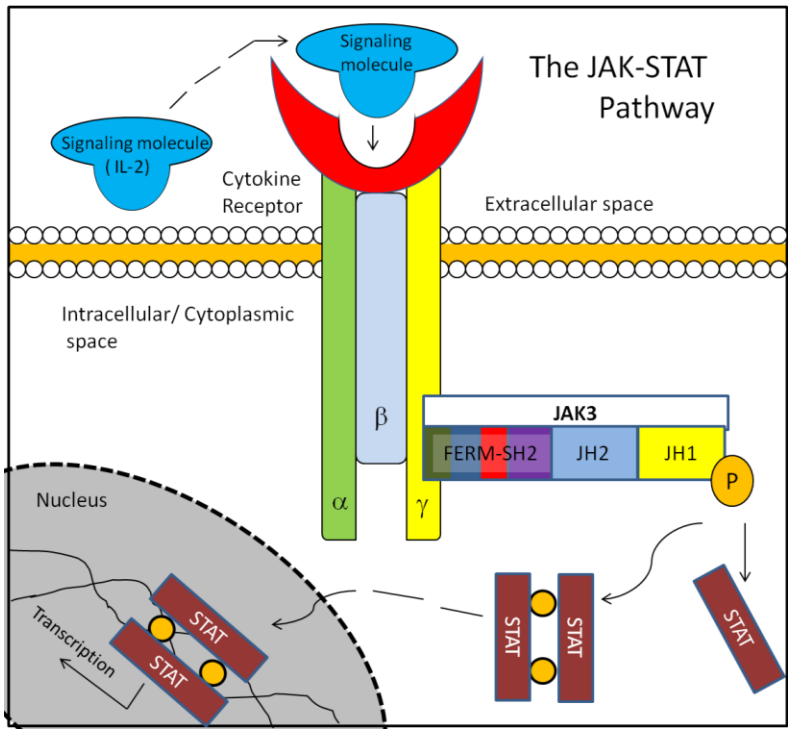

Figure 2. JAK-STAT (Janus Kinase- Signal Transducer and Activator of Transcription) signaling pathway.

As kinase proteins, the main activity of the JAKs within this pathway is phosphorylation, in which the JAK transfers a phosphate group from ATP or another energy-rich molecule to a separate protein substrate, subsequently causing activation of the phosphorylated protein. To activate itself, the JAK may also undergo auto-phosphorylation, where inter-residue transfer of a phosphate group occurs within the protein (Chrencik, & et. al, 2010). In the case of *tyrosine* kinases, such as the JAKs, the phosphate group is transferred to specific tyrosine residues, located in the kinase domain.

The JAK-STAT pathway is initiated with the binding of signaling molecules to extracellular portions of receptors on the cell surface (Wu & Sun, 2011). Signaling molecules, such as cytokines, interferons, interleukins, or hormones, are released into the extracellular space

by other cells to communicate cellular production needs. Since many of the various type I and II cytokine receptors that the JAKs interact with do not possess enzymatic kinase activity of their own, receptors must rely on JAKs to initiate the signal transduction cascade (Giordanetto & Kroemer, 2002). Upon receptor binding to the extracellular portion of the receptor, the intracellular receptor-associated JAK binds to the cytoplasmic tail of receptor (Wu & Sun, 2011). JAK-receptor binding induces JAK autophosphorylation and subsequent JAK activation. Binding of a STAT (Signal Transducer and Activator of Transcription) protein to the activated JAK ensues and JAK protein phosphorylation and activation of the STAT protein occurs (Wu & Sun, 2011).The activated STAT then continues the transduction of the cellular signal by dimerizing and entering the nucleus of the cell. Within the nucleus, the STAT binds to promoter regions on the DNA, promoting transcription of certain genes for the proliferation, maturation, and differentiation of cells (Giordanetto & Kroemer, 2002).

Hematopoietic Stem Cells and Signaling

The JAK-STAT pathway is used by a wide variety of cytokine signaling including granulocyte colony-stimulating factors, thrombopoietin, interferons, erythropoietin, and interleukins (IL) (Boggon & et. al., 2005). The different JAKs interact with different receptors within the pathway and therefore mediate an assortment of cellular processes. JAK1, JAK2, and TYK2 are expressed ubiquitously in different cell types, while JAK3 is predominately expressed in and mediates the development of hematopoietic stem cells (HSCs) (Chrencik & et. al, 2010). HSCs differentiate to form the different blood and immune cells within the body. Therefore properly functioning JAK3 protein is crucial for the proper development of these cells and the upkeep of a healthy immune system. (Hematopoietic Stem Cells, 2011). When we are well, the body has a relatively stable amount of immune cells and red and white blood cell production is

regulated with great precision. However, during infection, levels of HSCs fluctuate, and their self-renewal and maturation is controlled with interleukins and other signaling growth factors.

Interleukin 2 (IL-2) is the principal growth factor in regulating T-lymphocyte proliferation as well as the magnitude and duration of T-cell immune response following antigen encounter (Zhu & *et. al.*, 1997). One of the most well-known interactions of JAK3 within the JAK-STAT pathway is the protein's association with the interleukin-2 (IL-2) cytokine receptor (Zhu & *et. al.*, 1997). Antigen recognition stimulates release of IL-2 growth factor cytokines, which interact with the IL-2 receptors on immune cell surfaces to signal for the increased production of T-cells. Receptor binding initiates intracellular JAK3 binding to the cytoplasmic tail of the common gamma chain (γc) of the IL-2 receptors and subsequent signal transduction ensues resulting in increased immune cell production.

If JAK3 structure is mutated and function becomes aberrant, HSC signaling within the JAK-STAT pathway will become disfunctional and abnormal HSCs will be produced. JAK3's interactions within the JAK-STAT pathway therefore make it an important component for the proliferation, differentiation, and apoptosis of HSCs and link the protein to a number of immune-mediated processes.

Abrogating and Activating Mutations

A number of mutations have been identified in JAK3 that have been directly linked to various immune deficiency diseases, inflammatory diseases, cancers, leukemias, and myeloproliferative disorders. Figure 3 depicts the locations of various mutations for severe combined immunodeficiency (SCID) and acute megakaryoblastic leukemia (AMKL) in JAK3.

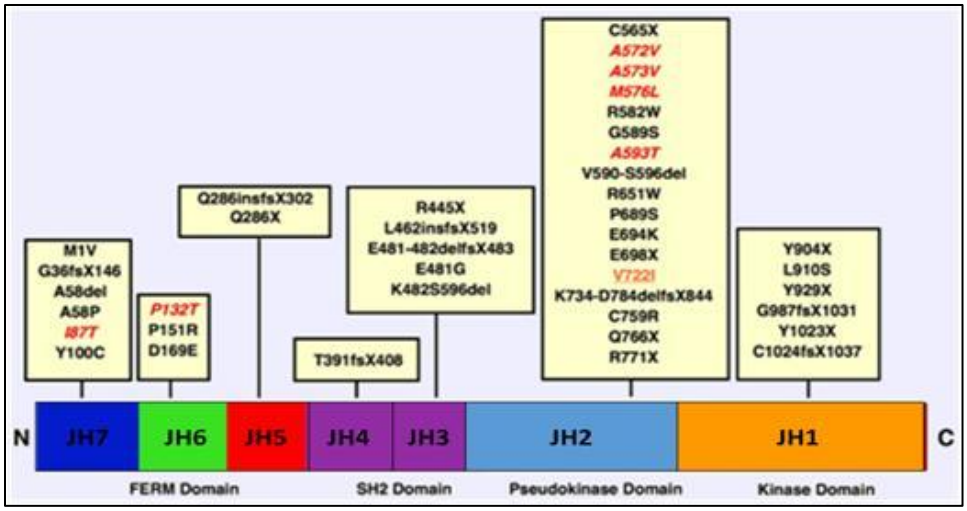

Figure 3. Mutations found in SCID (black), AMKL (red), and both diseases (orange) (Shi, & Amin,2007).

Patients experiencing various immune deficiency syndromes, characterized by insufficient or abnormal immune and blood cell circulation within the body, displayed mutated JAK3 with impaired function. One of the most studied of these immune deficiency diseases is the autosomal recessive form of Severe Combined Immunodeficiency Disease (SCID) (Vihinen, et. al., 2000). If there is an inhibiting mutation in JAK3, abrogating its activity, like is seen in SCID, the signals sent by cells calling for the increased production of immune cells to fight off infection will only get so far within the JAK-STAT pathway before they are impeded. In SCID, decreased JAK-STAT functionality results in the production of abnormal B cells and a decreased production of T-cells and NK cells necessary for cell-mediated immunity (Vihinen, et. al., 2000). This therefore leads to an increase in infections that characterize SCID and many of the immune deficiency diseases as seen in patients with JAK3 abrogating mutations.

One study analyzing SCID patient-derived and artificial mutations within the FERM domain of JAK3, showed that mutations within this domain impaired kinase-receptor interaction,

abrogated catalytic activity, and blocked ATP binding (Zhou et. al. 2001). Coimmuno-precipitation experiments in the same study utilizing JAK3 wild-type and mutant FERM and kinase domains showed that though both types associated, only wild-type FERM domain increased kinase activity (Zhou et. al. 2001). These studies suggest mutations in domains other than the catalytically active kinase domain, especially the FERM domain, may affect the overall function of the protein via domain-domain modulation.

Activating mutations within JAK3, like we see in AMKL, acute T-cell lymphoblastic leukemia (T-ALL), and other myeloproliferative disorders, deregulate the activity of the protein, and more immune or blood cells than necessary are produced. Additionally, many of these extraneous cells are improperly produced and without function, and may accumulate in the body causing problems that characterize these diseases. Patients with adult T-cell leukemia/lymphoma (ATLL), were shown to have mutations in the FERM domain of JAK3 which caused increased IL-2 signaling phosphorylation of STAT5A and gain of function in the kinase domain of JAK3 (Elliott, *et. al.* 2011). By comparing the JAK3 FERM domain to homologous FAK protein domain, this study also suggested FERM intramolecular contact with the kinase domain.

Much evidence suggests a link between JAK3 and many immune mediated diseases, yet the structural mechanisms behind the interactions, especially at the molecular level, are poorly understood. Though much is known about the protein's function within cellular signaling pathways, comprehensive information regarding the mechanisms and interactions at the molecular level remain inadequate since there is a lack of structural data concerning JAK3. It is known that the kinase domain of JAK3 is responsible for the catalytic activity of the protein. However, as suggested by mutagenesis studies, other domains, specifically the FERM domain, may interact and modulate the kinase domain function by regulating catalytic activity (Boggon,

2005). A full model encompassing all JAK3 domains will provide greater insight into the different domain functions, domain-domain modulations, and overall structure-function interactions of the protein.

CHAPTER II

METHODS

The structure of the kinase domain, JH1, of JAK3 was previously elucidated (Goedken, 2014). Methodology to predict the remaining FERM (JH7-JH5), SH2 (JH3-JH4), and pseudokinase (JH2) domains was employed using multi-template homology modeling and molecular dynamics simulations. JH2 and SH2-FERM domains were modeled separately, each utilizing a template structure from a JAK protein with highly conserved sequence homology to JAK3. Domain models were optimized and merged in phases, one domain at a time, using molecular dynamics simulations to produce two full models of JAK3, encompassing all domains. Validation of models was accomplished with root-mean square deviation (RMSD) calculations, energy minimization calculations, and identifying key residues important to functionality in our models and verifying their interactions.

Protein structure prediction: Homology Modeling

Protein structure may be predicted by various methods. Classically, protein structure is elucidated experimentally via x-ray crystallography or NMR spectroscopy. Though x-ray crystallography produces a higher resolution model of protein structure, it also requires the protein to be crystallized. Purification of a protein sample and subsequent crystallization is difficult for some larger protein families. The protein's crystalline structure may also vary from its solution structure. This is especially true for proteins that are water-soluble by removing a source of important intermolecular interactions. Further, crystallization only gives a snapshot of the protein, when in reality a protein is actually very dynamic and frequently undergoing conformational changes. NMR methodology of protein structure prediction analyzes the protein

in solution, mitigating many of the above-mentioned issues associated with crystallization. Structural data obtained from NMR frequently supplements theoretical modeling of a protein structure by providing additional information regarding residue-residue interactions. However, obtaining NMR structural information for protein is limited by size. Therefore, in this study computational theoretical modeling of protein structure was utilized to give a more comprehensive and dynamic picture of protein structure for JAK3, a relative large protein with 1124 residues.

The three-dimensional structure of JAK3, a relatively large protein (1124 residues), was generated using computational multi-template homology modeling techniques and MD simulations, to produce a tertiary model comprising all domains (JH1-7). Since the primary amino acid sequence of a protein is directly related to its structure and therefore function, the rationale behind homology modeling is that proteins with highly conserved sequences also have conserved structure and overall function (Karadaghi, 2015). Therefore, this method utilizes proteins with known structures and conserved sequence homology with respect to a target protein, as templates to model the unknown structure of a target protein. Separate models for the different domains were generated using different templates and then combined using two different pathways. Molecular dynamics simulations were used to generate multiple probable model structures at each phase.

Generation of JAK3 domain models

For ease of modeling, due to the large size of the JAK3 protein and in order to better conserve homology among domains, models of the JH2 (pseudokinase domain), and the JH3-JH7 regions (SH2-FERM domain), were constructed separately.

Homology among JAKs: Multiple Sequence Alignments

In general, proteins within the same family are grouped together due to highly conserved homology. Sequence homology within the JAK family was confirmed in order to determine if the different JAK family proteins would be suitable templates for JAK3 modeling. Sequences of JAK1, JAK2, JAK3, and TYK2 from various species were obtained from the NCBI Gene Database using BLAST (Basic Local Alignment Search Tool) (Altschul, 1990) (Table 1).

Table 1. JAK family protein sequences obtained from NCBI BLAST. Accession version (gi) ID number given for each sequence used on NCBI website.

Jak 1	Jak2	Jak3	Tyk2	Band 4.1 proteins *Homo sapiens*
Homo sapiens ID: P23458.2	*Homo sapiens* ID: O60674.2	*Homo sapiens* ID: P52333.2	*Homo sapiens* ID: AAH14243.1	Ezrin ID: NP_003370.2
Pan troglodytes ID: JAA44554.1	*Pan troglodytes* ID: JAA41169.1	*Cyprinus carpio* ID: AAF24169.1	*Pan troglodytes* ID: JAA43378.1	Radixin ID: AAA36541.1
Danio rerio ID: AAH47165.1	*Mus musculus* ID: EDL41674.1	*Mus musculus* ID: Q62137.2	*Mus musculus* ID: AAY21060.1	Moesin ID: NP_002435.1
Rattus norvegicus ID: EDL97824.1	*Siniperca chuatsi* ID: ACU12481.1	*Rattus norvegicus* ID: NP_036987.2	*Sus scrofa* ID: CAG15148.1	B4.1 ID: P11171.4
Bos taurus ID: DAA31301.1	*Tetraselmis* ID: JAC84248.1	*Gallus gallus* ID: NP_990327.1	*Bos taurus* ID: DAA27926.1	
	Xenopus laevis ID: NP_001085288.3		*Xenopus laevis* ID: NP_001085663.1	

In order to determine homology among the sequences collected, the sequences were aligned in pairwise sequence alignments (PW) and multiple sequence alignments (MSA) using NCBI BLAST, CLUSTAL OMEGA (Sievers, et. al, 2011), and EMBOSS Needle (Rice, et. al, 2000) online analysis tools. In a sequence alignment, an algorithm is used to match up similar amino acid residues among two or more protein sequences. Sequences may be shifted forward or backward from one another or broken up into different sections, creating gaps within the

sequence, with the ultimate goal of aligning as many identical or similar residues among the sequences as possible. The alignment produced depicts the residues and gaps conserved among the sequences. Similarity values are also generated, translating those conserved residue properties into quantitative percentages that reveal the overall homology among the protein sequences.

The full sequences of JAK1, JAK2, JAK3, and TYK2 from the species listed in Table 1 (excluding Band 4.1 proteins) were aligned in an MSA using the CLUSTAL OMEGA tool on the EMBL-EBI (European Molecular Biology Laboratory-European Bioinformatics Institute) website (Sievers, 2011). The CLUSTAL OMEGA program operates using the Hhalign algorithm to identify and maintain conserved residue properties (Soding, 2005). By comparing the entire sequence of each protein, encompassing all domains, the results of the full MSA were used to determine which JAK protein was most similar to JAK3 overall, among all domains.

In a separate MSA, the homology of the JH2 domain among the JAK proteins was investigated by aligning only the JH2 portions of the sequences of JAK1, JAK2, JAK3, and TYK2 from Table 1. The purpose of aligning just the JH2 portions was to give a more precise alignment of conserved residues among the proteins with respect to only the JH2 domains. Similarity value results from the JH2 domain-specific MSA revealed which JAK protein had the most homologous JH2 domain to the JH2 domain of JAK3.

Similarly, one more MSA was created aligning only the SH2-FERM domains of JAK family proteins (Table 1) to ascertain the JAK with the most similar SH2-FERM domain to that of JAK3. This MSA included the Band 4.1 proteins listed in Table 1 since the FERM domain is structurally very similar to the domains associated with this protein (Girault, *et. al.,* 1999).

Identification of Structural Templates

The different MSAs produced gave varying similarity values revealing which JAK proteins would be most suitable for use as templates for JAK3 domain models. The next step was to search the RCSB protein data bank (PDB) for available domain structures of the most homologous JAKs (Berman, et. al., 2000). Structural templates for each of the JH2 and SH2-FERM domains were then chosen based on highest MSA similarity values to the respective JAK3 domain, availability on the PDB, and highest resolution model.

Pairwise Alignments

With templates chosen, a PW was completed for each the JH2 and SH2-FERM domains aligning the JAK template with the respective JAK3 domain. Since residue alignments shift depending on the sequences involved, the PW was completed in order to obtain one more possible alignment of sequences, with the possibility of creating an alignment with increased conserved residue properties. The EMBOSS (European Molecular Biology Open Software Suite) Needle program on the EMBL-EBI website was used to perform the pairwise alignment (Rice & et. al, 2000). The Needle program utilizes the Needleman-Wunsch algorithm to perform a global alignment, which, when compared to local alignment programs, allows for more query cover, aligning the most residues without truncating residues from the ends of the sequences.

Generation of domain models

Homology models of the JH2 domain and SH2-FERM domain were generated using the MODELLER 9.17 program (Sali, A. and Bundell, T. L., 1993). The program essentially takes the residues from a template sequence with a structure and substitutes the residues from a target sequence (JAK3) into the template structure, thereby creating a rough structural model of the target sequence. In order to do this, the program requires an alignment of the template and target

sequences of the same length. During the MSA and PW alignments, sequences were shifted to increase conservation of residues, creating gaps in the sequences in the process. Therefore the template sequence in the full MSA, domain-specific MSA, and PW sequence alignments for each domain, had to be modified accordingly to diminish these gaps, ensuring proper alignment of conserved residues and identical sequence length. Residues were deleted from the template when a gap was aligned in the corresponding location on the target sequence. Gaps appearing on the template sequence were inserted with aligned residues from the target sequence. The biopolymer function on the SYBYL X 2.0 program (Certara Inc.) was then used to update the PDB structure file of the template to reflect the modifications made to its sequence.

MODELLER 9.17 was used to create 5 rough structural models of each the JH2 and SH2-FERM domains of JAK3 for each the full MSA, domain-specific MSA, and PW alignments. For each domain, the theoretical models produced from each alignment were superimposed with respect to their template structure and root-mean square deviation (RMSD) calculations were performed using visual molecular dynamics visualization program (VMD) (Humphrey,W.Dalke, A., and Schulten, K, 1996). Results from RMSD calculations revealed which structural models produced, deviated the least from its template. The theoretical models with the least structural deviations were chosen as the initial model for each domain and were subsequently optimized.

Molecular dynamics simulations

JAK3 domain models were optimized with all-atom molecular dynamics (MD) simulations in solvent environment (Figure 4) using the Nanoscale Molecular Dynamics (NAMD) Program (Phillips, 2005). A summary of simulation details is shown in Table 2.

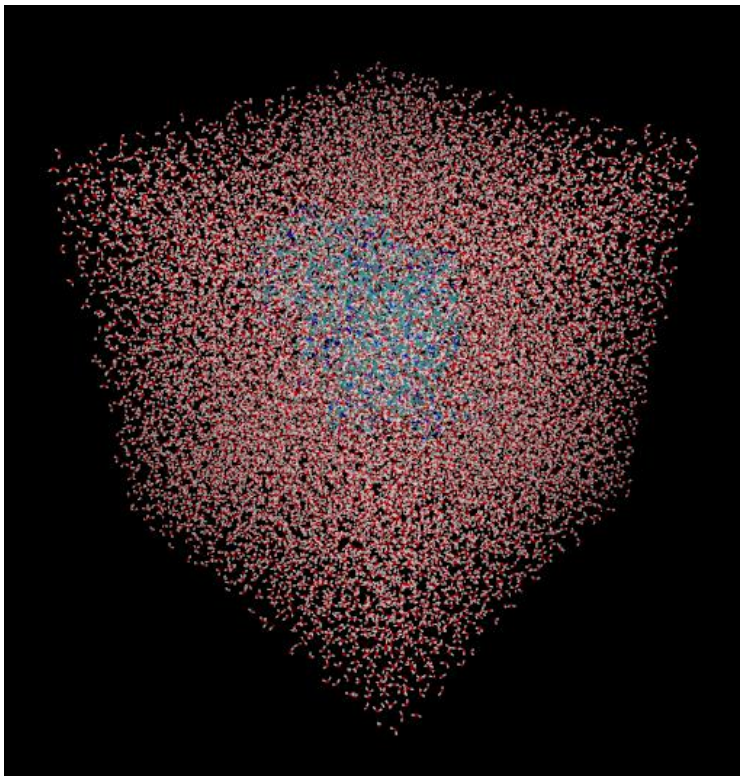

Figure 4. Depiction of the JH2 domain model solvated with water box padding for sample simulation setup.

Table 2. MD simulation details for JH2 and SH2-FERM domains individually and each subsequent merge of domains.

	Number of total atoms	Number of solvent molecules	Cell dimensions (L x W x H) (Angstroms)	Simulation times (ns)
JH1	36420	10692	70.3 x 70.3 x 70.3	10
JH2	55705	17119	77.7 x 77.7 x 77.7	10
SH2-FERM	79643	24068	91.3 x 91.3 x 91.3	12
(JH2)-(SH2-FERM) merge	262869	83695	136 x 136 x 136	17
(JH1)-(JH2) merge	174,700	55336	124 x 124 x 124	10
(JH1-JH2)-(SH2-FERM) merge	253896	79255	150 x 150 x 150	underway
(JH1)-(JH2-SH2-FERM) merge	253896	79255	150 x 150 x 150	underway

All model systems were initially minimized to remove bad interactions using conjugate gradient minimization algorithm within NAMD. The solvated systems were initially equilibrated at 0.5 fs timestep, 300 K and 1 atm pressure in the NPT ensemble using the Nose-Hoover Langevin piston pressure control. The Langevin piston Nose-Hoover method in NAMD is a combination of the Nose-Hoover constant pressure method (Martyna & et. al., 1997) with piston fluctuation control implemented using Langevin dynamics (Feller & et. al., 1995). After equilibration, production run was carried out using Langevin dynamics (Kubo et. al., 1991). Total simulation times for each system are also shown in Table 2. All structural analyses were based on the total production trajectory with a collection interval of 1.0 ps. The Charmm 36 forcefield (Best, R.B., 2012) was used for all protein simulations.

For each system, structures obtained from the NVT MD simulation were clustered based on their RMSD values relative to the beginning structure as reference. Energy minimization calculations were performed on each representative structure from each cluster in order to determine the lowest energy model to be used for each domain. Chosen optimized models of the individual domains were then used to assemble a full structural model of JAK3 using additional MD simulations. Assembly of the full model was accomplished in phases, combining one domain at a time in different orders for a total of two pathways generating two full probable models. The rationale behind merging the domains in different orders was to allow the domains to interact with one another in multiple ways, allowing an improved search of the conformational space.

Structural Analysis

For the different models, domain-domain interactions were quantified by calculating hydrogen-bonding interactions and salt-bridge interactions for the trajectories. Hydrogen

bonding interaction (short- and medium-range) between residues were calculated using 5.0 angstroms cutoff distance between the donor (D) atom and the acceptor (A) atom and 20^{o} <ADH angle cutoff. Salt bridge interactions were calculated by determining the distance between oxygen atoms of acidic residues and nitrogen atoms of basic residues with a cutoff distance of 3.2 Å.. Domain-domain modulation and interaction was expounded upon by highlighting key residues within the protein. Residues were highlighted that are known to have a distinct effect on the overall functionality of the protein when mutated along with tyrosine residues at catalytically active phosphorylation sites. Inter-domain proximity of these functional residues indicated interaction among domains. Quantifying the distance between interacting residues validated known domain-domain interactions and new information about domain function and residue interaction within the protein among domains.

Computational Resources

All molecular dynamics simulations were carried using an Intel x86-64 Linux cluster with 852 compute nodes at the Texas A&M University High Performance Research Computing Facility (College Station, TX). All system setup and data analyses were performed using AMD-based workstations.

CHAPTER III

RESULTS & DISCUSSION

Homology and Template data

MSA and PW alignments provided sequence similarity values of the JAK proteins to JAK3, used to identify structural domain templates for modeling. Table 3 presents a summary of similarity values from each of the three MSAs created, revealing the similarity between human JAK1, JAK2, and TYK2 with respect to JAK3.

Table 3. MSA and PW sequence alignment similarity value data. Asterisk (*) designates alignment and JAK template protein chosen for each domain.

Alignment	Percent similarity of templates to JAK3		
	JAK1	JAK2	TYK2
JH2-domain specific MSA	45.52%	**57.09%***	45.90%
SH2-FERM specific MSA	34.21%	39.65%	**33.47%***
Full MSA	42.06%	49.45%	40.82%
Domain Pairwise	N/A	56.9%	31.4%

Across all sequence alignments, JAK2 had the highest similarity to JAK3. Therefore with the highest sequence homology, JAK2 was determined to be the best candidate to be used as the template for modeling the JH2 and SH2-FERM domains of JAK3. However, when the RCSB protein data bank was searched for JAK2 domain structures, only structures for the JH2 domain of JAK2 were available, while SH2-FERM domain structures of the protein were not yet accessible. The JAK2 JH2 structure with PDBID: 4FVR was chosen with the highest resolution

available at the time (2.0A) (Bandaranayake, 2012). SH2-FERM domain structures for JAK2 (PDBID: 4Z32) and JAK1 (PDBID: 5IXI) did not become available until 6/22/2016 and 5/18/2016 respectively (McNally, 2016; Ferrao, 2016). Therefore, of the JAK proteins, the only available structure of the SH2-FERM domain at the time the domain models were generated was from the TYK2 protein (PDBID: 4PO6) (Wallweber, 2014). The TYK2 structure of SH2-FERM also had better resolution (1.99A) than this domain structure for JAK1 (2.57A) and JAK2 (3.04A). Therefore the SH2-FERM domain structure of TYK2 was chosen as the template for modeling the corresponding domain in JAK3.

The structure of the JH1 domain, already previously elucidated, was chosen for use in our model from the list of available structures on the PDB based on highest resolution of available structures at the time of the experiment. At the time, PDBID: 3LXL and PDBID: 4QPS were the highest resolution structures of JH1 available of 1.74A and 1.8A respectively. The 3LXL structure was not chosen as the representative structure of JH1 to be used in our model since it was a complex of JAK1, TYK2, and other compounds. Therefore, the 4QPS structure was chosen for the JH1 domain of JAK3 to use in our model (Goedken, 2015). A summary of structural domain templates chosen for use in our model is depicted Table 4.

Table 4. JAK proteins chosen as structural templates for the domains of JAK3 obtained from the RCSB protein data bank.

Domain	PDBID	JAK protein	Resolution	Date Released	Reference
JH1	4QPS	JAK3	1.8 A	01/14/15	Goedken, 2015
JH2	4FVR	JAK2	2.0 A	07/25/12	Bandaranayake, 2012
SH2-FERM	4PO6	TYK2	1.99 A	04/02/14	Wallweber, 2014

RMSD and Energy minimization validation

Following the identification of structural templates, Modeller 9.17 was used to create 5 rough structural models of each of the domains, one of which was chosen for each domain based on lowest RMSD values to be used for further optimization. Backbone RMS deviation of chosen SH2-FERM model from TYK2 template (PDBID: 4PO6) was 4.94 angstroms. Backbone RMS deviation of chosen JH2 model from JAK2 template (PDBID: 4FVR) was 2.06 angstroms.

Models selected for each domain were minimized and optimized using MD simulation in solvent environment and analyzed for structural deviation with RMSD trajectory calculations. Figures 5 & 6 depict RMSD values for the simulations of the JH2 domain model and SH2-FERM domain model respectively using the first frame as the reference structure.

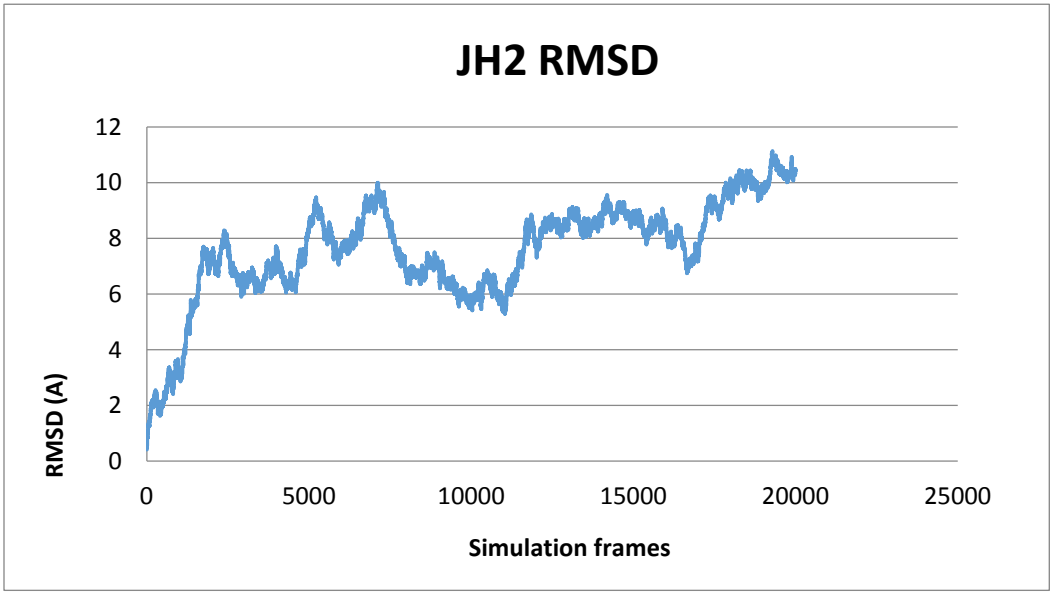

Figure 5. RMSD values of optimized JH2 domain model with respect to original template structure over the course of the MD simulation. Each frame represents a snapshot of the structure of the JH2 model where increasing frame number corresponds to increasing amount of time the protein model was run at 300K (NVT). RMSD values presented in units of Angstroms (Å).

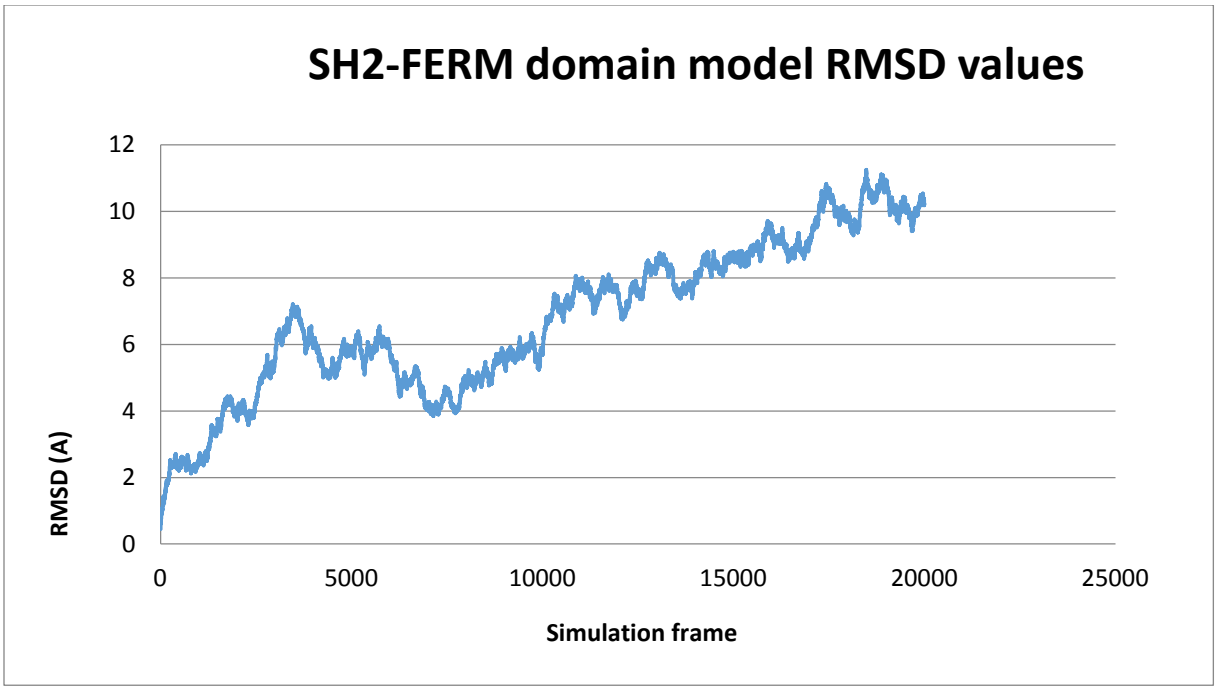

Figure 6. RMSD values of optimized SH2-FERM domain model with respect to original template structure over the course of the MD simulation. Each frame represents a snapshot of the structure of the SH2-FERM model where increasing frame number corresponds to increasing amount of time the protein model was run at 300K (NVT). RMSD values presented in units of Angstroms (Å).

RMSD trajectory plots show clustering of structures at certain values. Structures were selected from each RMSD value cluster underwent additional energy minimization. Energy minimization calculations (Table 5) were performed on each structure to determine the lowest energy domain model.

Table 5. Results from energy minimization calculations for each the JH2 and SH2-FERM models. Energies presented as relative energies with respect to lowest energy model.

Frame (JH2 structure)	**Relative energies (kcal/mol)**		**Frame (SH2-FERM structure)**	**Relative Energies (kcal/mol)**
625	107.0241		1000	382.0698
1380	199.1805		2000	491.3359
2050	399.7004		2900	348.9356
3600	157.1997		3500	97.0701
4800	210.4949		4400	323.9464
6200	184.994		5000	156.2752
7100	188.2698		6500	40.5313
8500	298.2372		7300	63.6948
10000	359.419		8300	342.1475
13500	35.8906		10500	147.2586
16800	179.0692		11600	24.4063
17500	167.8347		13000	0
18500	0		13700	61.9413
19300	140.2411		15000	192.0517
19900	137.7126		15900	253.749
			17500	182.1309

Lowest energy domain models selected were used subsequently in building the merged models, JH2-JH1 model and FERM-SH2-JH2 model. Independent MD simulations were carried out for each of the merged structures. For each model, the trajectories were clustered based on their RMSD values relative to a reference structure. RMSD data in Figure 7 (JH1-JH2 merge) and Figure 8 (JH2-SH2-FERM merge). A representative structure from each cluster was subjected to energy minimization to compare the models obtained. Energy minimization results in Table 6 for each merged model.

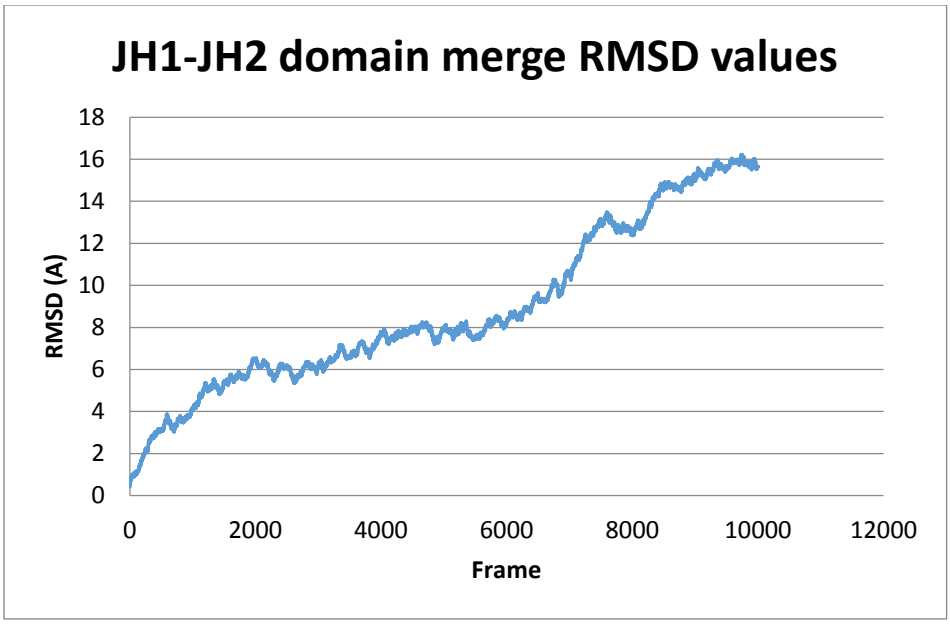

Figure 7. RMSD values of the optimized model of the JH1 domain merged with the JH2 domain over the course of the MD simulation with respect to the beginning structure of the model before MD simulation ensued. Each frame represents a snapshot of the structure of the JH1-JH2 merged model where increasing frame number corresponds to increasing amount of time the protein model was run at 300K (NVT). RMSD values presented in units of Angstroms (Å).

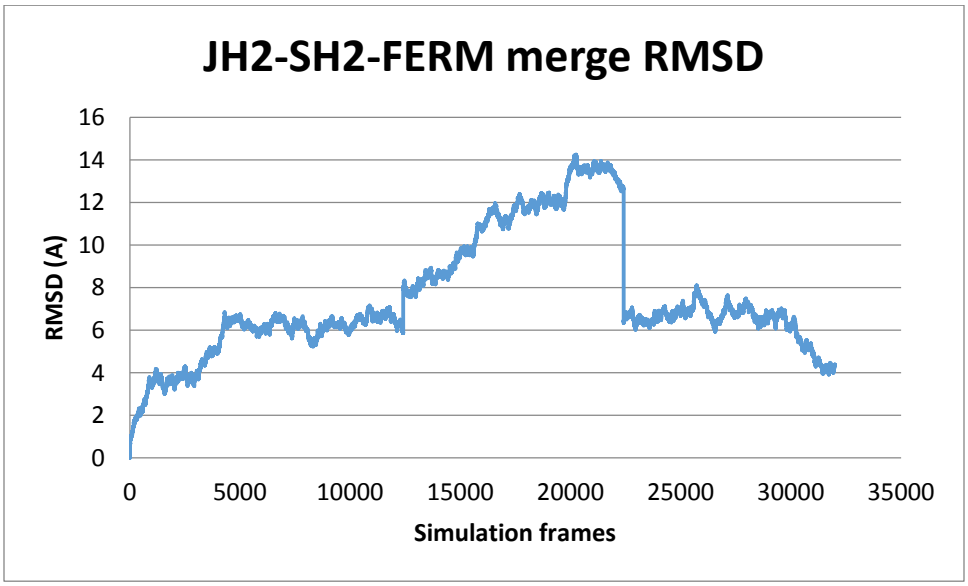

Figure 8. RMSD values of the optimized model of the JH2 domain merged with the SH2-FERM domain over the course of the MD simulation with respect to the beginning structure of the model before MD simulation ensued. Each frame represents a snapshot of the structure of the JH2-SH2-FERM merged model where increasing frame number corresponds to increasing amount of time the protein model was run at 300K (NVT). RMSD values presented in units of Angstroms (Å).

Table 6. Results from energy minimization calculations for each the JH1-JH2 merged model and JH2-SH2-FERM merged model. Energies presented as relative energies with respect to lowest energy model for each simulation.

Frame (JH1-JH2 merge structure)	**Relative energies (kcal/mol)**		**Frame (JH2-SH2-FERM merge structure)**	**Relative Energies (kcal/mol)**
1398	114.0333		15473	279.4626
1807	18.2943		13710	584.1231
2826	230.0102		19104	377.4947
3613	128.2497		17215	597.6278
4413	147.097		21287	211.9521
5232	61.3441		21380	0
6156	71.5865		24124	244.8753
6809	124.9345		32204	36.5425
7368	74.6408		33826	272.0179
7570	181.1973		34531	238.3733
7629	58.4832		35436	359.3718
7980	0		37205	396.6667
8547	70.1507		38588	284.8
9670	124.2963		40548	545.3102
			42205	471.5956
			43120	572.7942
			46083	427.7317
			44371	362.0231

Generation of Full Structural Model

The assembly of the full model of JAK3 was accomplished in several phases. Two pathways were utilized to generate the full model (Figure 9).

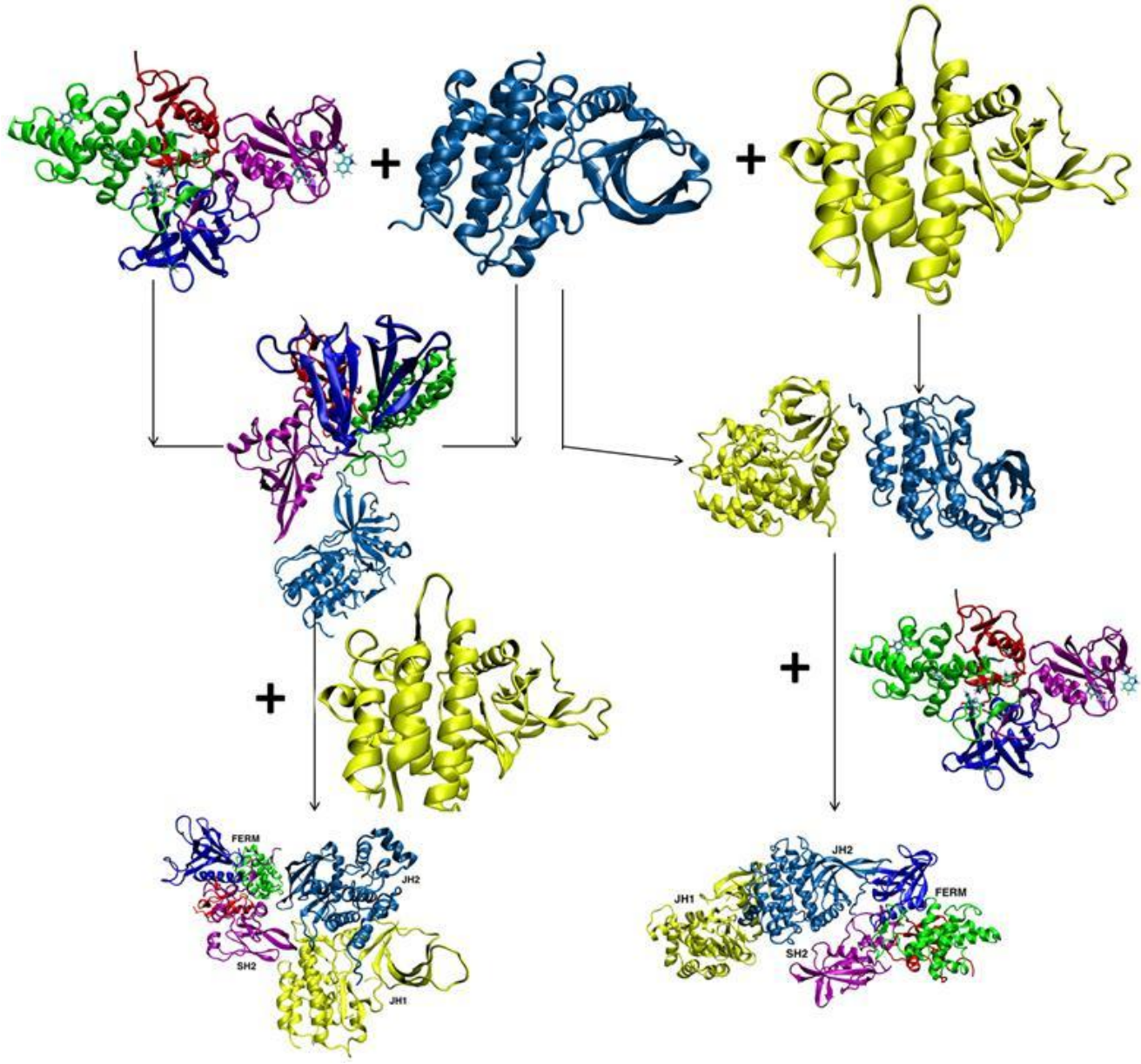

Figure 9. Two visual pathways depict the manner in which domains of JAK3 were merged into two full models. Domain colors depicted as follows: JH1 kinase domain (yellow), JH2 pseudokianse domain (Light blue), SH2 domain (purple), and FERM domain with lobes A, B,

and C (red, green, blue respectively). The structure for the JH1 domain depicted was obtained from the PDB (PDBID: 4QPS) and further optimized with MD simulation for use in our full model. The JH2 and FERM domains were generated using methodology described.

In the first path, the JH1 domain (PDBID: 4QPS) was merged with the JH2 domain by orienting the end sequence of the JH2 domain with the start of the JH1 domain. The system was then solvated and subjected to similar MD simulation procedure described in methodology but with longer simulation times (Table 2). RMSD trajectories from the simulations were clustered and representative structures (without water molecules) were minimized similar to the methods above. The selected structure/s were merged with the SH2-FERM domain model followed by similar optimization procedures described.

In the second path, the SH2-FERM domain was merged with the JH2 domain in a separate series of MD simulations (Table 2). Further, the JH1 domain was merged with the JH2-SH2-FERM model (Table 2). All simulations parameters, clustering methods, and selection of most probable structure/s were the same for the two paths. This resulted in two full models of JAK3 comprising all domains depicted in Figure 9.

Structural Analyses of the Models

FERM-SH2-JH2 model.

The FERM-SH2 model (Figure 10) obtained resembles the typical structural motifs, alpha helical structures and β-strand structures of a FERM domain consisting of three major lobes, A, B, and C (Giordanetto & Kroemer, 2002; Hamada, et. al., 2000). In the model structures, Y100 is shown in the interior core of the FERM domain. Y100C mutation has been

correlated with SCID, which can be correlated to structural destabilization of the FERM lobes with the mutation. SH2 (or SH2-like domain) consists of β-strands and an α-helical structure.

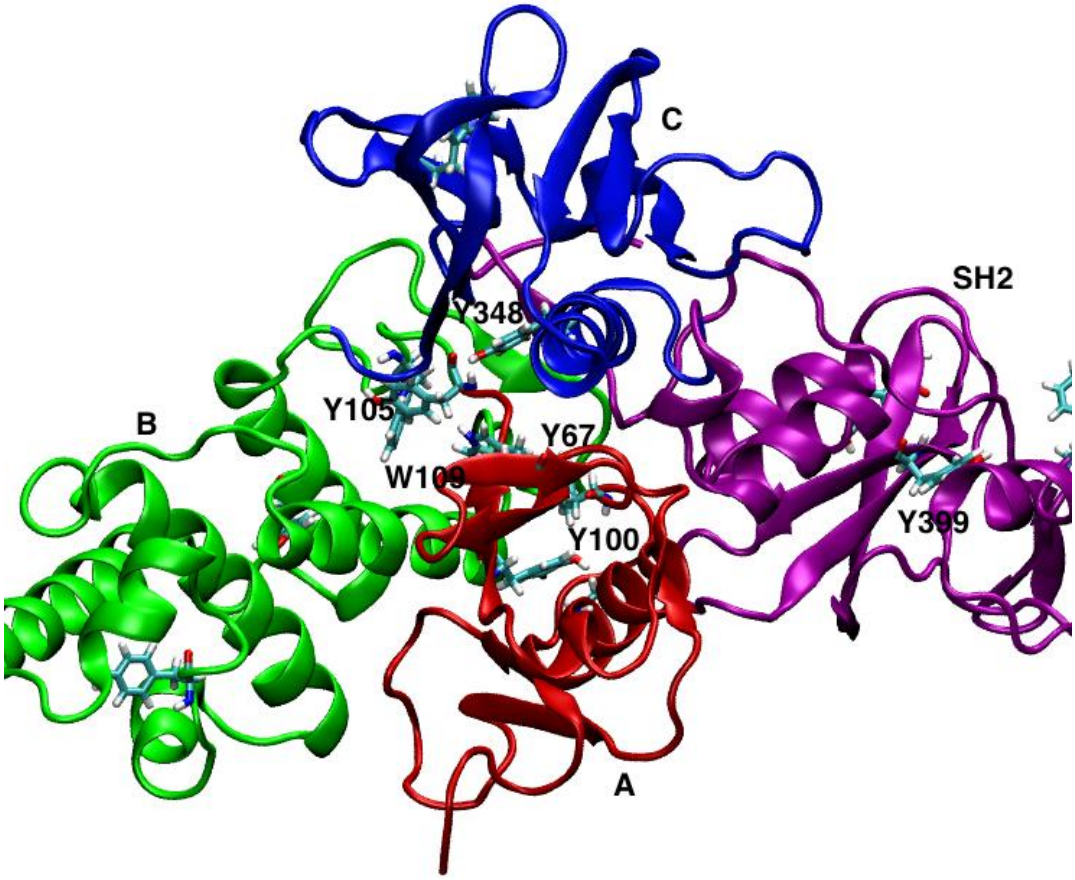

Figure 10. FERM-SH2 model with FERM lobes A (red), B (green), and C (blue), and SH2 (purple) depicting key secondary structures and key residues are highlighted.

The organization of the FERM-SH2 domains is stabilized by both short-range and long-range salt-bridge and hydrogen bonding interactions (summarized in Table 7). Residues depicted in FERM-SH2-JH2 model in Figure 11.

Table 7. Summary table of hydrogen-bonding and salt bridge interactions at domain interfaces in JAK3 model.

Domain Interface	Interaction				
FERM-SH2	**Hydrogen Bonding**		**Salt Bridges**		
	Residues		Residues	Average distance (Angstroms)	Distance Range (Angstroms)
	H116---H492	R121---D383	D294---R490	6.37	3.26 to 12.52
	C115---R490	R117---R490	D276---R490	8.54	3.35 to 14.23
SH2-JH2	D383---E547	T381---E547	D383---R549	4.43	3.30 to 6.47
	Y425---R657				
FERM-JH2			R121---E522	9.09	3.30 to 6.47
			R121---E547	6.46	3.84 to 9.40
JH2-JH1	S779---P814	D784---E819	E786---R899	4.19	3.09 to 10.49
	S779---I816	D776---Y886			

Hydrogen bond interactions and electrostatic interactions were analyzed between the two domains. The key hydrogen-bond and salt-bridge interactions include H492 (SH2) and H116 (FERM), R121 (FERM) and D383 (SH2), C115 (FERM) and R490 backbone (SH2), R117 (FERM) and R490 backbone (SH2). The hydrogen-bonding interactions showed occupancies >60 % throughout the entire simulation. A prominent long-range electrostatic interaction is shown between D276 (FERM) and R490 (SH2), and D294 (FERM) and R490 (SH2), with an average salt-bridge distance of 8.54Å and 6.37 Å throughout the simulation respectively. Mutation of these residues will likely cause disruption in the interaction network. The hydrogen-bonding and salt-bridge analyses were carried out for every 5000 frames of the trajectories collected.

The interface between the SH2 domain and the JH2 domain is characterized by many hydrogen-bonding and salt-bridge interactions summarized in Table 7 and depicted in Figure 11.

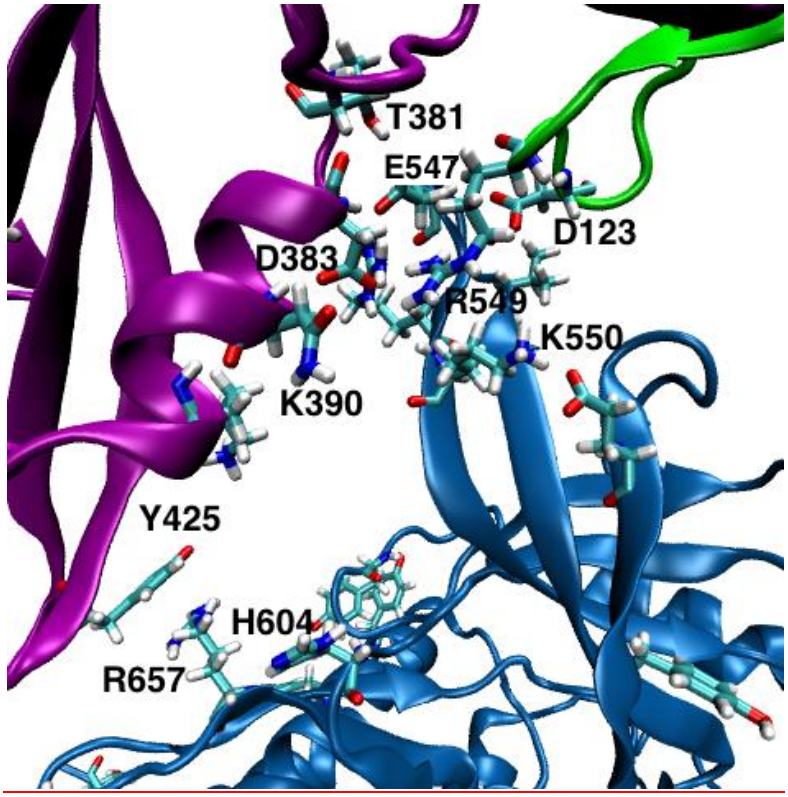

Figure 11. Key residue interactions highlighted on JH2, SH2, and FERM domains.

Key hydrogen-bonding interactions occur between D383 (SH2) and E547 (JH2) as well as between T381 (SH2) and E547 (JH2), which exhibited ~80% hydrogen-bonding occupancy through the simulation. A close interaction was also observed between Y425 (SH2) and R657 (JH2) but is only present ~ 10% of the time. The JH2 and FERM-SH2 domains also showed salt-bridge interactions between D383 (SH2) and R549 (JH2), D522 (JH2) and R121 (FERM) , E547 (JH2) and R121 (FERM), with average distances of 4.43, 9.09, 6.46 angstroms, respectively.

JH1-JH2 model

As shown in Figure 12, there are a few key residues that line the JH2-JH1 interface. A summary of hydrogen-bonding and salt bridge interactions is recorded in Table 7.

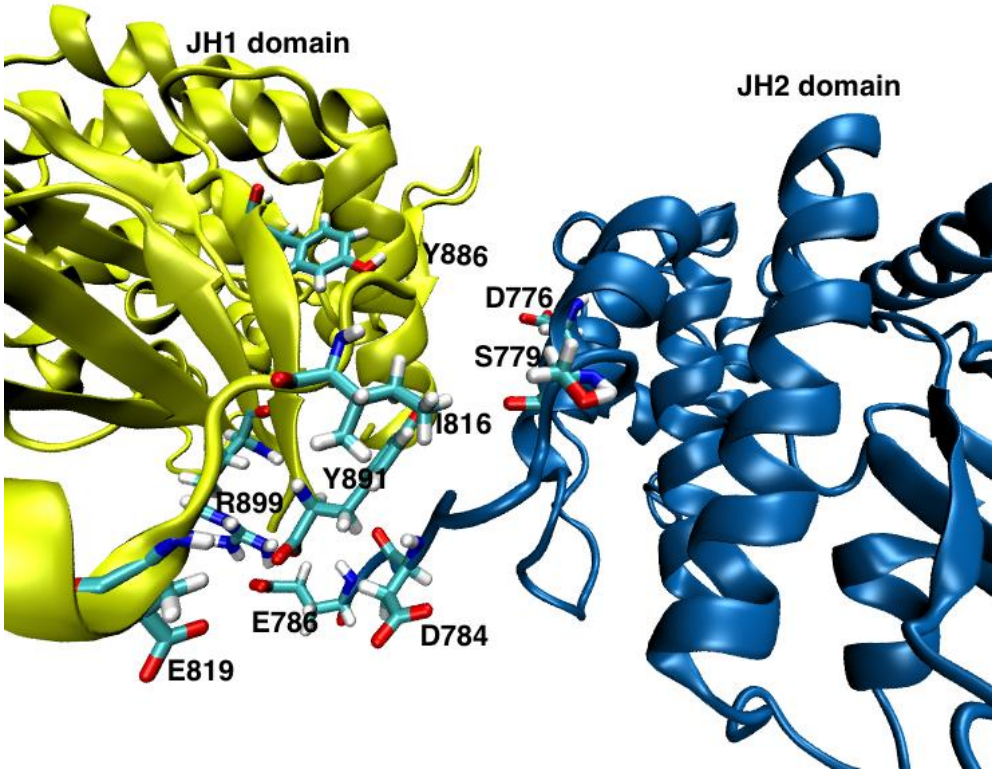

Figure 12. Key residue interaction between residues on JH2 and JH1 domains highlighted.

Based on analysis of the trajectories, stable hydrogen bonding interactions (59.3-70% occupancies) were observed between S779 backbone (JH2) and P814 backbone (JH1), D784 (JH2) and E819 (JH1), I816 (JH1) and S779 (JH2), D776 and Y886. Stable salt-bridge interactions are exhibited by E786-R899, which are most likely similar to the case exhibited in JAK2 in a previous study (Shan, Y., 2014). In JAK2, mutation of these residues showed an auto-inhibitory effect.

CONCLUSION IV

Two probable models of the JAK3 protein are reported, though further optimization and validation of the models is necessary. The confidence that our model is most probable is validated in many ways throughout our methodology. Beginning with template selection, templates were chosen based on highest homology to JAK3 using three different alignments of sequences in order to ensure most accurate conserved residue properties. Selected template structures therefore were already very similar to JAK3 structure, exemplified by relatively low RMSD values for each domain after Modeller 9.17 was used to produce rough models. RMSD structural validation and lowest energy minimization validation of domain models at each subsequent merge phase, supported that models selected at each phase had lowest structural deviation and energy. Relatively long simulation times allowed sampling of the conformational space and provided various low energy stable model structures. Merging the models using two different pathways also provided the possibility of different interactions and orientations of domains. Structural deviations between these models must be analyzed further to ensure one most probable model for JAK3. Further validation of the models verifying functionally significant residues demonstrated inter-domain interactions of JH2 and SH2-FERM along with JH1 and JH2. Key residue interactions have also been identified in the models. Mutagenesis studies (beyond the scope of this study) on those key residues will be an interesting endeavor to see how those affect the structure and function of JAK3.

Broader Impacts: Inhibitor Potential

Due to the observed link between JAK3 and various immune diseases, JAK3 has been targeted for the development of selective therapeutic compounds to inhibit JAK3 in patients with

activating mutations. The idea behind selective inhibitors is to target the specific biological molecule of interest and inactivate only that molecule for a period of time in order to abrogate its activity, having less far-reaching side effects than broader treatments such as chemotherapy. Depending on the structural specificity of the drug to the target molecule, the inhibitor may inhibit other molecules with similar structure causing unwanted side-effects. As of now, the design of JAK3 inhibitors developed (Goedken & et. al., 2015; Meyer & et. al., 2010; Jaime-Figueroa & et. al., 2013) has been limited to targeting just the kinase domain of JAK3. The comprehensive model of our protein gives greater insight into the structure-function mechanisms of the protein and may aid in developing more selective inhibitors with greater specificity through structure-based drug design.

REFERENCES

Altschul, Stephen F., Gish, Warren, Miller, Webb, Myers, Eugene W., and Lipman, David J. (1990). Basic local alignment search tool. *J. Mol. Biol. 215,* 403-410.

Bandaranayake, R.M., Ungureanu, D., Shan, Y., Shaw, D.E., Silvennoinen, O., & Hubbard, S.R. (2012). Crystal structures of the JAK2 pseudokinase domain and the pathogenic mutant V617F. *Nat.Struct.Mol.Biol., 19:* 754-759. doi: 10.1038/nsmb.2348.

Best, R.B., Zhu, X., Shim, J., Lopes, P.E.M., Mittal, J., Feig, M., and MacKerell Jr., A.D. (2012). Optimization of the additive CHARMM all-atom protein force field targeting improved sampling of the backbone phi, psi and side-chain chi1 and chi2 dihedral angles. *Journal of Chemical Theory and Computation,* 8: 3257-3273. PMC3549273

Berman, H. M., Westbrook, J., Feng, Z., Gilliland, G., Bhat, T. N., Weissig, H., Shindyalov, I. ., & Bourne, P. E. (2000). The Protein Data Bank. *Nucleic Acids Research*. 28 (1): 235-242. doi: https://doi.org/10.1093/nar/28.1.235.

Boggon, T. J., Li, Y., Manley, P. W., & Eck, M. J. (2005). Crystal structure of the Jak3 kinase domain in complex with a staurosporine analog. *Blood.* 106(3): 996-1000.

Chrencik, J. E., Patny, A., Leung, I. K., Korniski, B., Emmons, T. L., Hall, T., Weinberg, R. A., Gormley, J. A., Williams, J. M., Day, J. E., Hirsch, J. L., Kiefer, J. R., Leone, J. W., Fischer, H. D., Sommers, C. D., Huang, H., Jacobsen, E. J., Tenbrink, R. E., Tomasselli, A. G., & Benson, T. E. (2010). Structural and Thermodynamic Characterization of the TYK2 and JAK3 Kinase Domains in Complex with CP-690550 and CMP-6. *Journal of Molecular Biology.* 400, 413-433. doi:10.1016/j.jmb.2010.05.020.

Elliott N. E., *et. al.* (2011) FERM domain mutations induce gain of function in JAK3 in adult T-cell leukemia/lymphoma. *Blood* 118(14):3911-21.

Feller, S. E., Zhang, Y., Pastor, R. W., & Brooks, B. R. (1995). Constant pressure molecular dynamics simulation: The Langevin piston method. *J. Chem. Phys. 103*(11).

Figueroa, J. S., De Vicente, J., Hermann, J., Jahangir, A., Jin, S., Kuglstatter, A., Lynch, S. M., Menke, J., Niu, L. Patel, V. Shao, A., Soth, M., Vu, M. D., Yee, C. (2013). Discovery

of a series of novel 5H-pyrrolo[2,3-b]pyrazine-2-phenyl ethers, as potent JAK3 kinase inhibitors. *Bioorganic & Medicinal Chemistry Letters*. *23*: 2522-2526.

Ferrao, R., Wallweber, H.J., Ho, H., Tam, C., Franke, Y., Quinn, J., & Lupardus, P.J. (2016). The Structural Basis for Class II Cytokine Receptor Recognition by JAK1. *Structure.* 24(6): 840-842. doi: org/10.1016/j.str.2016.03.023.

Giordanetto F. & Kroemer T. (2002) Prediction of the structure of human Janus kinase 2 (JAK2) comprising JAK homology domains 1 through 7. *Protein Engineering* 15(9):727-37.

Goedken, E.R., Argiriadi, M.A., Banach, D.L., Fiamengo, B.A., Foley, S.E., Frank, K.E., George, J.S., Harris, C.M., Hobson, A.D., Ihle, D.C., Marcotte, D., Merta, P.J., Michalak, M.E., Murdock, S.E., Tomlinson, M.J., & Voss, J.W. (2015) Tricyclic Covalent Inhibitors Selectively Target Jak3 Through an Active-site Thiol. *J.Biol.Chem*. *290*: 4573-4589. doi: 10.1074/jbc.M114.595181.

Goedken, E. & et. al. (2014). Tricyclic Covalent Inhibitors Selectively Target Jak3 through an Active Site Thiol. *The Journal of Biological Chemistry, 290,* 4573-4589. doi: 10.1074/jbc.M114.595181.

Girault, J. A., Labesse, G., Mornon, J. P., Callebaut, I. (1999). The N-termini of FAK and JAKs contain divergent band 4.1 domains. *Trends in Biochemical Sciences.* 24(2): 54-57. doi: http://dx.doi.org/10.1016/S0968-0004(98)01331-0.

Hamada K., Shimizu T., Matsui T., Tsukita S., & Hakoshima T. (2000). Structural basis of the membrane-targeting and unmasking mechanisms of the radixin FERM domain. *EMBO Journal*, *19*(17):4449-62. doi: 10.1093/emboj/19.17.4449.

Hematopoietic Stem Cells (2011). *Stem Cell Information*. Retrieved from http://stemcells.nih.gov/info/scireport/pages/chapter5.aspfx

Humphrey, W., Dalke, A. and Schulten, K., (1996). VMD - Visual Molecular Dynamics. *J. Molec. Graphics*, *14*: 33-38.

Karadaghi S, A (2015). Introduction to Homology Modeling. *Homology Modeling.* Retrieved from http://www.proteinstructures.com/Modeling/homology-modeling.html.

Kubo R., Toda M., Hashitsume N., (1991). Statistical Physics II: Nonequilibrium Statistical Mechanics. *31*(2). *Springer Series in Solid-State Sciences.* doi: 10.1007/978-3-642-58244-8.

Martyna, G. J., Tobias, D. J., and Klein, M. L. (1994). Constant pressure molecular dynamics algorithms. *J. Chem. Phys, 101*(5).

Meyer, D. M., Jesson, M. I., Li, X., Elrick, M. M., Funckes-Shippy, C. L., Warner, J. D., Gross, C. J., Dowty, M. E., Ramaiah, S. K., Hirsch, J. L., Saabye, M. J., Barks, J. L., Kishore, N., and Morris, D. L. (2010). Anti-inflammatory activity and neutrophil reductions mediated by the JAK1/JAK3 inhibitor, CP-690,550, in rat adjuvant-induced arthritis. *Journal of Inflammation.* doi: 10.1186/1476-9255-7-41.

McNally, R., Toms, A.V., & Eck, M.J. (2016). Crystal Structure of the FERM-SH2 Module of Human Jak2. *PLoS ONE.* 11(5): e0156218. doi:10.1371/journal.pone.0156218.

Phillips, J. C., Braun, R., Wang, W., Gumbart, J., Tajkhorshid, E., Villa, E., Chipot, C., Skeel, R. D., Kale, L., & Schulten, K (2005). Scalable molecular dynamics with NAMD. *Journal of Computational Chemistry*, 26:1781-1802.

Rane S., G. & Reddy E., P. (2000). Janus kinases: components of multiple signaling pathways. *Oncogene.* 19(49): 5662-5679.

Rice, P., Longdena, I., Bleasbyb, A. (2000). EMBOSS: The European Molecular Biology Open Software Suite. *Trends in Genetics.* 16(6): 276-277. doi: org/10.1016/S0168-9525(00)02024-2.

Šali, A. and Blundell, T., L. (1993). Comparative protein modeling by satisfaction of spatial restraints. *J. Mol. Biol. 234*: 779-815.

Shi, P. & Amin, H. M. (2007). JAK3 (Janus Kinase 3 or Just Another Kinase 3): Atlas of Genetics and Cytogenetics in Oncology and Haematology. *AminDepartment of Hematopathology, The University of Texas MD Anderson Cancer Center.*

Shuai, K. & Liu, B. (2003) Regulation of JAK–STAT signaling in the immune system. *Nature Reviews Immunology* 3:900-911. doi:10.1038/nri1226.

Sievers, F., Wilm, A., Dineen, D., Gibson, T. J., Karplus, K., Li, W., Lopez, R., McWilliam, H., Remmert, M., Söding, J., Thompson, J. D., & Higgins, D. G. (2011). Fast, scalable generation of high-quality protein multiple sequence alignments using Clustal Omega. *Molecular Systems Biology, 7:* 539. doi:10.1038/msb.2011.75

Söding, J. (2005) Protein homology detection by HMM–HMM comparison. *Bioinformatics* 21: 951-960.

Vihinen, M., *et. al*. (2000) Molecular Modeling of the Jak3 Kinase Domains and Structural Basis for Severe Combined Immunodeficiency. *Clinical Immunology, 96*(2):108-18.

Wallweber, H.J.A., Tam, C., Franke, Y., Starovasnik, M.A., & Lupardus, P.J. (2014). Structural basis of IFN receptor recognition by TYK2. *Nat.Struct.Mol.Biol. 21*(5): 443-448. doi: 10.1038/nsmb.2807.

Wallweber, H.J.A., Tam, C., Franke, Y., Starovasnik, M.A., & Lupardus, P.J. (2014). Crystal structure of the human TYK2 FERM and SH2 domains with an IFNAR1 intracellular peptide. *Nat. Struct. Mol. Biol.* doi: 10.2210/pdb4po6/pdb

Wu, W. & Sun, X. (2011) Janus kinase 3: the controller and the controlled. *Acta Biochim Biophys Sin, 44*(3): 187-196.doi: 10.1093/abbs/gmr105.

Zhou, Y. & et. al. (2001) Unexpected Effects of FERM Domain Mutations on Catalytic Activity of Jak3:Structural Implication for Janus Kinases. *Molecular Cell* 8(5):959-69.

Zhu, M., Berry, J. A., Russell, S. M., & Leonard, W. J. (1997) Delineation of the Regions of Interleukin-2 (IL-2) Receptor b Chain Important for Association of Jak1 and Jak3. *The Journal of Biological Chemistry.* 273(17): 10719-10725. doi: 10.1074/jbc.273.17.10719.